Millimeter-Wave Uniform Amplitude SIW Series Power Divider for 2D Leaky-Wave Antenna Arrays

Weiguang Song*, George Goussetis†, Lei Wang‡,
*Institute of Sensors, Signals and Systems, Heriot-Watt University, EH14 4AS Edinburgh, United Kingdom.
ws2032@hw.ac.uk, wanglei@ieee.org

***Abstract*—This paper proposes a millimeter-wave uniform amplitude substrate integrated waveguide (SIW) series power divider for 2D leaky-wave antenna arrays, which is built by connecting 10 elaborately designed unit cells in series. The unit cell consists of an SIW to slot and microstrip line coupling structure, which can be further extended to a low-cost phase shifter by introducing varactors or other active components. Theoretical analysis is made firstly to specify the necessary conditions for uniform amplitude power division. Then, a short via is added to the unit cell to meet the admittance condition. A full wave simulation is conducted to extract the normalized admittance and transmission characteristics of the unit cell, which provides useful references for the design of geometric parameters. After the design of unit cells, a 1-to-10 SIW series power divider is implemented by connecting unit cells with aimed transmission characteristics. At last, comparisons are made between the uniform amplitude power divider and the non-uniform amplitude power divider to demonstrate the feasibility of the design method. The proposed uniform amplitude SIW series power divider for 2D leaky-wave antennas works between 24 GHz and 29 GHz, which is competitive for millimeter-wave communication and wireless power transfer systems.**

***Index Terms*—Leaky-wave antenna array, millimeter-wave, power divider, substrate integrated waveguide (SIW), uniform amplitude.**

I. Introduction

Millimeter-wave leaky-wave antennas have been receiving great interests due to the rapid development and widespread application of the 5th generation (5G) communication and artificial intelligence and internet of things (AI-IOT) [1]-[3]. Compared to traditional phased arrays, leaky-wave antennas are able to steer the beam directions by simply changing the frequency of the input source, saving the complex and expensive active feeding networks, especially the cost of phase shifters [4]-[5]. Meanwhile, millimeter-wave has the inherent advantage of rich spectrum resource, making its combination with leaky-wave antennas a very competitive solution for future mobile communication and wireless power transfer systems (WPT) [6]-[7]. Typically, leaky-wave antennas are in the form of slot arrays on the surface of rectangular waveguides or substrate integrated waveguides (SIW). By designing the shape of the slot, either linearly polarized or circularly polarized waves can be transmitted [8]-[9].

However, in leaky-wave antennas, the radiating amplitude of each slot attenuates gradually along the wave propagation direction within the wavguide and the phase difference between each slot is dependent on the frequency, limiting the flexibility of the beamforming. Especially for purely passive 2D leaky-wave antenna arrays, with frequency being the only variable, the beam direction is limited to the diagonal line of the array geometry, as shown in Fig. 1. To maximize the two-dimensional beamforming capacity, the amplitude and phase of the power divided to each antenna unit should be independently controllable. This can be approached by introducing an active feeding network as shown in Fig. 1. The active feeding network can control the amplitude and phase of the wave entering each leaky-wave antenna unit, making two-dimensional beam scanning in any angles possible for the 2D array. The simplest active feeding network only introduces an varactor to the feeding port of each leaky-wave antenna unit. The capacity of the varactor can be controlled by changing the voltage loaded on it, resulting in changed phase difference for fixed input power source. The amplitude of the power divided to the antenna units can be controlled by specially designed passive components.

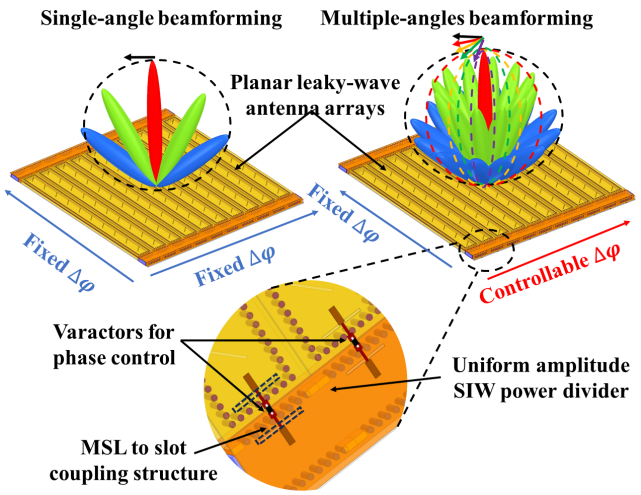

Fig. 1. 2D leaky-wave antenna arrays with single-angle and multiple-angles beamforming.

With the purpose of implementing such an active feeding network as discussed above, this paper firstly proposes a 1-to-10 uniform amplitude SIW series power divider. The transmission characteristics of the unit cell is analyzed to provide references for the parameter adjustments of each individual

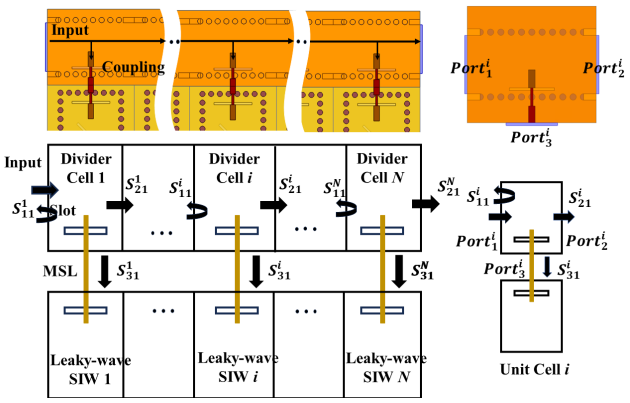

Fig. 2. Power flow within the SIW series power divider and the unit cell.

unit cell. Then, all unit cells with different and specifically designed transmission characteristics are connected in series to construct the entire power divider. The proposed uniform amplitude SIW series power divider in this paper works in the frequency range from 24 GHz to 29 GHz, which almost covers the entire 5G NR bands, n257 (26.5 GHz−29.5 GHz), n258 (24.25 GHz−27.5 GHz) and n261 (27.5 GHz−28.35 GHz). It has the potential to be extended to an active uniform amplitude power divider in the following study for millimeter-wave 2D leaky-wave antenna arrays.

II. Theoretical Analysis

There has already been some previous study on rectangular power dividers [10]-[12], providing some basic ideas for the design of SIW power dividers. As shown in Fig. 2, the proposed uniform SIW amplitude power divider consists of N unit cells connected in series. Each of the unit cells absorbs equal portion of power from the input and then transfers it to the SIW leaky-wave antenna unit. In this study, the unit cell is conducted using the coupling structure of slot and microstrip line (MSL). Each unit cell can be analyzed as a three-port device marked with $Port_1^i$, $Port_2^i$ and $Port_3^i$, representing power input port, power output port and power coupling port, respectively [13]-[15]. As all the leaky-wave antenna unit shares same parameters, they are replaced with ideal waveports in the analysis so that the transmission characteristics of the unit cells can be extracted more accurately. In the S-parameter matrix of the i_{th} cell, S_{11}^i represents the power reflected to the $(i-1)_{th}$ cell, S_{21}^i represents the power transmitted to the $(i+1)_{th}$ cell, S_{31}^i represents the power coupled to the i_{th} SIW leaky-wave antenna unit. For the N_{th} unit cell, S_{21}^N represents the power transmitted to the matched port at the end of the power divider. To implement the uniform power allocation and non-reflection transmission, the following conditions are required:

$$|S_{11}^i|^2 = 0, \tag{1}$$

$$|S_{21}^i|^2 = \frac{N-1}{N-1+i}, \tag{2}$$

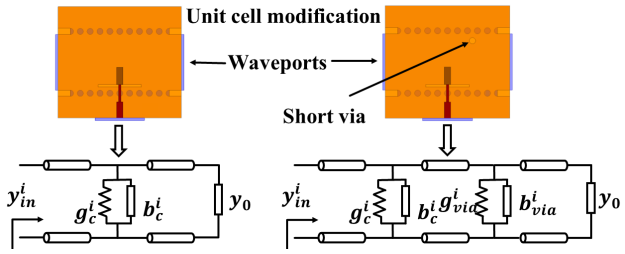

Fig. 3. Equivalent circuits of unit cells with and without the short via.

$$|S_{31}^i|^2 = \frac{1}{N-1+i}. \tag{3}$$

The transmission characteristics of the SIW-Slot-MSL unit cell can be effectively analyzed using the equivalent circuit shown in Fig. 3 [16]. The normalized admittance of the SIW-Slot-MSL coupling structure y_c^i can be calculated by:

$$y_c^i = g_c^i + jb_c^i, \tag{4}$$

where g_c^i and b_c^i represent the conductance and susceptance of the coupling structure, respectively. For a well-matched waveport which feeds the SIW, the normalized admittance should be:

$$y_0 = 1. \tag{5}$$

Thus, for the coupling structure to meet (1), y_c^i should meet the following condition:

$$g_c^i = y_0 = 1, \tag{6}$$

$$b_c^i = 1. \tag{7}$$

To meet (2) and (3) for the uniform amplitude power division, y_c^i should meet the following condition:

$$y_c^i = g_c^i = \frac{1}{N-1+i}. \tag{8}$$

However, (6) and (8) can not be met simultaneously. Thus, a modification is made to the unit cell by introducing a short via between the coupling structure and the output port. The normalized admittance y_{total}^i of the SIW-Slot-MSL coupling structure with short via can be calculated by:

$$y_{total}^i = y_c^i + y_{via}^i = g_c^i + jb_c^i + g_{via}^i + jb_{via}^i, \tag{9}$$

where y_{via}^i, g_{via}^i and b_{via}^i represent the admittance, conductance and susceptance of the short via, respectively. Thus, with (8), condition (1)-(3) can be met by:

$$g_{via}^i = \frac{N-1}{N-1+i}, \tag{10}$$

$$b_c^i + b_{via}^i = 0. \tag{11}$$

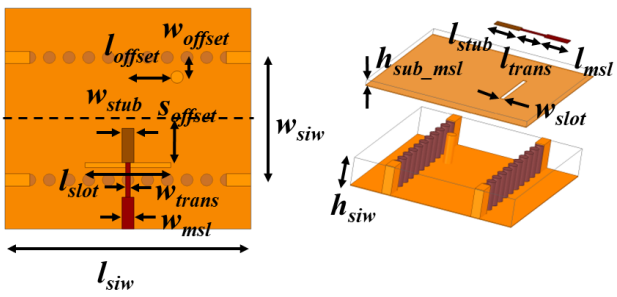

Fig. 4. Geometry of the SIW power divider unit cell.

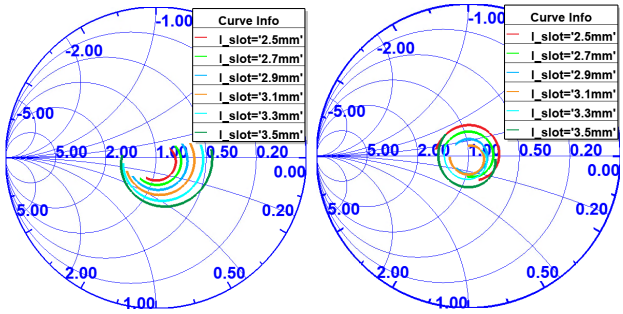

(a) (b)

Fig. 5. Normalized input admittance mapping of unit cells with and without short via. (a) Without short via, (b) with short via.

As can be concluded from the analysis, the admittance of the coupling structure and short via of each unit cell should be different, requiring the parameters of each unit cell to be calculated and designed separately.

III. Unit Cell Design

To precisely extract the admittance of the coupling structure, a full wave simulation of the unit cell as shown in Fig. 4 is conducted in Ansys HFSS. The normalized input admittance of the unit cell seen at the input port y_{in}^i can be calculated by:

$$y_{in}^i = \frac{1 - S_{11}^i}{1 + S_{11}^i}. \tag{12}$$

Then, the input admittance of the coupling structure can be obtained by subtracting the normalized admittance of the output waveport from the y_{in}^i, which can be expressed by:

$$y_{total}^i = y_{in}^i - 1. \tag{13}$$

To build the SIW-Slot-MSL coupling structure, an SIW working from 24 GHz to 30 GHz is designed using a Rogers 4003C board, of which the thickness, dielectric constant and loss tangent are 1.524 mm, 3.55 and 0.0027, respectively. A slot offset 1.8 mm from the center of the SIW is curved on the top copper surface to enable the power coupling. A Rogers 4003C board with the thickness of 0.305 mm is stacked over the SIW board to support the MSL. The MSL consists of three sections, an open-ended stub with around a quarter wave-length to short the MSL to ground, a 50 ohm transmission line with arbitrary length for connection with active components, and a transition with around a quarter wave-length to transform the impedance of the slot to that of the 50 ohm transmission line. The initial value of the unit cell sizes are given in Table I. While tuning the admittance of the coupling structure, the length and width of the slot, the stub and the transition MSL are swept to obtain the target conductance. Then, the position of the short via is swept to compensate for the normalized admittance to 1.

TABLE I
Parameters and Transmission Characteristics of Unit Cells

w_{siw}	l_{siw}	l_{slot}	w_{slot}	l_{msl}	w_{msl}
5.0 mm	8.0 mm	3.0 mm	0.2 mm	1.2 mm	0.5 mm
l_{trans}	w_{trans}	l_{offset}	w_{offset}	l_{stub}	w_{stub}
1.2 mm	0.2 mm	1.5 mm	0.3 mm	1.2 mm	0.5 mm

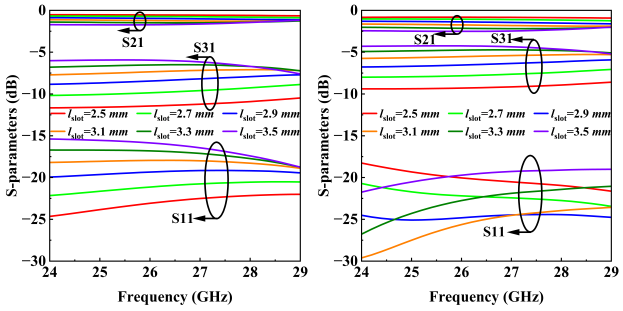

(a) (b)

Fig. 6. Transmission characteristics of unit cells with and without short via. (a) Without short via, (b) with short via.

The extracted normalized input admittance mappings of the unit cell with and without short via against the length of the slot are given in Fig. 5 as an example. In both cases, the normalized admittance of the unit cell changes with the length of the slot. However, for the unit cell without the short via, the radius of the admittance circles are large. Meanwhile, as the frequency changes from 24 GHz to 29 GHz, the admittance almost remains below the conductance line, always taking the state of capacitive susceptance. With the short via, the admittance of the unit cell from 24 GHz to 29 GHz is moved closer to the center of the admittance circle, and the values of the susceptance changes between inductive ones and capacitive ones, achieving a better matching performance.

Among all the variables, the length of the slot has the most significant effect on the value of admittance. Thus, with all other parameters being proper values firstly, the parameter sweeping of the slot length against the transmission characteristics is conducted to obtain references for the design of the uniform power divider. As shown in Fig. 6, the transmission characteristics represented by S-parameters of the unit cells against the length of the slot are compared between unit cells or and without the short via. In both cases, S31 of the unit cell increases with the length of the slot while S21 changes in a reverse trend. S11 of unit cells without the short via increases with the length of the unit cell, indicating that the shorter the

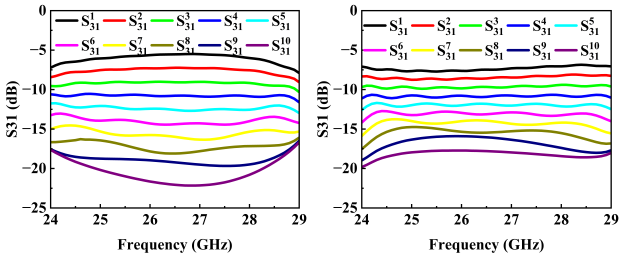

(a) (b)

Fig. 7. Power coupling characteristics of the non-uniform amplitude SIW series power divider (a) Without short via, (b) with short via.

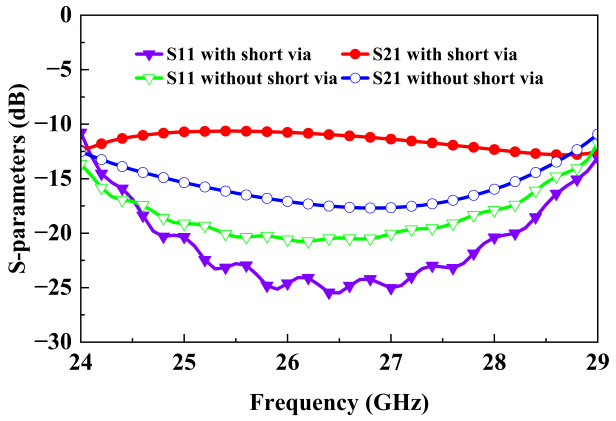

Fig. 8. S-parameters of the non-uniform amplitude SIW series power divider.

slot within the sweeping range, the less the reflection. S11 of unit cells with the short via decreases with the length of the slot when it is below 3.1 mm and then changes in the reverse trend. However, S11 of the unit cell with short via is always smaller than that of the unit cell without short via. In contrast, S31 of the unit cell with short via is always bigger than that of the unit cell without short via. Thus, conclusion can be made that the short via in the unit cell performs well in the suppression of reflection and improvement of power transmission.

IV. SIW Series Power Divider Design

A non-uniform amplitude SIW series power divider with 10 same unit cells without short via is built and analyzed

TABLE II
PARAMETERS AND TRANSMISSION CHARACTERISTICS OF UNIT CELLS

Cell No.	l_{slot} (mm)	l_{trans} (mm)	l_{offset} (mm)	g_c^iexp (S)	S31exp (dB)	S31ach (dB)
1	2.7	1.2	2.0	0.1	−10	−9.87
2	2.7	1.4	2.0	0.11	−9.54	−9.47
3	2.7	1.0	1.5	0.13	−9.03	−9.04
4	2.9	1.0	2.0	0.14	−8.45	−8.32
5	2.9	1.0	1.5	0.17	−7.78	−7.81
6	2.9	0.8	1.5	0.2	−6.99	−7.02
7	3.1	0.8	1.5	0.25	−6.02	−6.14
8	3.3	1.4	1.0	0.33	−4.77	−4.74
9	3.5	1.4	1.5	0.5	−3.01	−3.62
10	3.5	1.4	1.5	1.0	0	−3.62

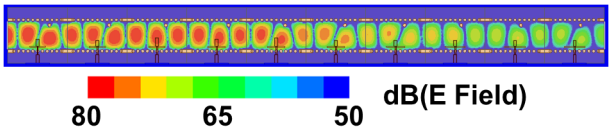

Fig. 9. E Field distribution inside the uniform amplitude SIW series power divider at 27 GHz.

firstly to quantify the power attenuation along the direction of the propagation, as shown in Fig. 7(a). The power coupled to the port 3 of each unit cell reduces exponentially from the first cell and the amount of the coupled power varies with the frequency. Then, short vias are added to the SIW power divider to demonstrate its matching performance, as shown in Fig. 7(b). Although the coupled power still attenuates exponentially, its variation with frequency is well suppressed. S11 and S21 parameters of the non-uniform power dividers with and without short vias are given in Fig. 8. The load of short vias effectively suppresses the power reflection represented by S11, enabling more power to be transmitted to matched port 2, which is represented by larger S21. This is promising for power dividers with more unit cells.

Then, a uniform SIW power series divider is built by elaborately designing the parameters of each unit cell. According to the theoretical analysis, unit cells with specific conductance values should be found firstly on the admittance mapping, then positions of short vias have to be found for each unit cell so that admittance balance can be achieved. However, this method is not efficient and takes a lot of repetitive work, which is only used to provide an instruction for the design. Instead of finding proper conductance values and then doing compensations one by one, S-parameters that represent the transmission characteristics are used to determine the geometric parameters of the unit cells.

As shown in Table II, parameters of unit cells that have significant effect on admittance are swept to get transmission characteristics mappings. Then unit cells with parameters that achieve specific values of admittance are used to obtain expected transmission characteristics. In this case, S31 is selected as the main transmission characteristics for reference. In the table, g_c^iexp, S31exp and S31ach represents the expected conductance, expected S31 and achieved S31 of the i_{th} unit cell, respectively. For the 10_{th} unit cell, the expected S31 should be 0, which is extremely difficult to achieve. Thus, same parameters are used for the 9_{th} and 10_{th} unit cell to approach the expected performance. As shown in Fig. 9, the E field inside the SIW power divider attenuates gradually as it propagates by each unit cell. S31 of the unit cells are plotted in Fig. 10. From the 1_{st} to the 8_{th} unit cell, S31 remains around -11 dB with the variation between ± 1.5 dB, demonstrating the feasibility of the design method. For the 9_{th} and the 10_{th} unit cells, the coupling coefficients are not large enough to obtain the same power as the former 8 unit cells. In practical applications, the two ports can be connected to matched loads instead of antenna units to prevent reflection and non-uniform

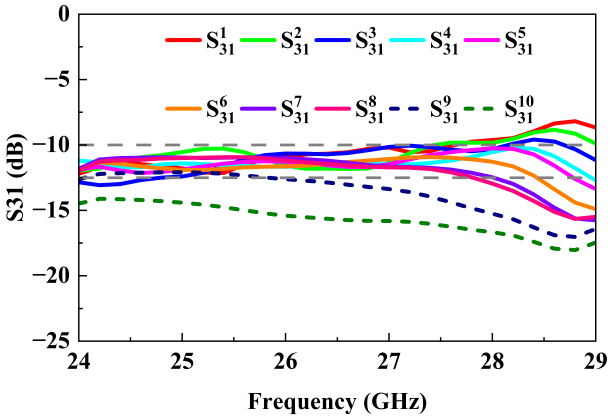

Fig. 10. Power coupling characteristics of the uniform amplitude SIW series power divider.

amplitude radiation distribution.

V. Conclusion

This paper presents a 1-to-10 uniform amplitude SIW series power divider for 2D leaky-wave antenna arrays. Theoretical analysis indicates that each unit cell of the power divider should be separately designed so that specific normalized admittance can be obtained for the expected power division ratio. A short via is added in each unit cell to compensate for the normalized admittance to be 1, so that a non-reflection transmission structure can be achieved. Among all the geometric parameters of the unit cell, some critical ones, such as the length of the slot, are swept to construct a mapping of the relationship between parameters and transmission characteristics. Then, the mapping is used to determine the parameters of the unit cells used for the uniform amplitude SIW series power divider. Comparisons between the uniform and non-uniform amplitude SIW series power divider demonstrate the feasibility of the entire design process. The uniform amplitude SIW series power divider is convenient for active component integration, so that low-cost beamformers for 2D leaky-wave antenna arrays can be implemented more easily and the space coverage efficiency of the array can be improved greatly, making it a competitive solution for millimeter-wave communication systems and WPT systems.

References

[1] L. Wang, J. L. Gómez-Tornero and O. Quevedo-Teruel, "Substrate Integrated Waveguide Leaky-Wave Antenna With Wide Bandwidth via Prism Coupling," in IEEE Transactions on Microwave Theory and Techniques, vol. 66, no. 6, pp. 3110-3118, June 2018.

[2] L. Chettri and R. Bera, "A Comprehensive Survey on Internet of Things (IoT) Toward 5G Wireless Systems," in IEEE Internet of Things Journal, vol. 7, no. 1, pp. 16-32, Jan. 2020.

[3] M. Wagih, G. S. Hilton, A. S. Weddell and S. Beeby, "Millimeter-Wave Power Transmission for Compact and Large-Area Wearable IoT Devices Based on a Higher Order Mode Wearable Antenna," in IEEE Internet of Things Journal, vol. 9, no. 7, pp. 5229-5239, 1 April1, 2022.

[4] L. Wang, J. L. Gómez-Tornero, E. Rajo-Iglesias and O. Quevedo-Teruel, "Low-Dispersive Leaky-Wave Antenna Integrated in Groove Gap Waveguide Technology," in IEEE Transactions on Antennas and Propagation, vol. 66, no. 11, pp. 5727-5736, Nov. 2018.

[5] L. Wang, J. L. Gómez-Tornero and O. Quevedo-Teruel, "Substrate Integrated Waveguide Leaky-Wave Antenna With Wide Bandwidth via Prism Coupling," in IEEE Transactions on Microwave Theory and Techniques, vol. 66, no. 6, pp. 3110-3118, June 2018.

[6] S. Rezaee, M. Memarian and G. V. Eleftheriades, "2D Dirac Leaky Wave Antenna with Circular Polarization for millimeter-wave applications," 2020 IEEE International Symposium on Antennas and Propagation and North American Radio Science Meeting, Montreal, QC, Canada, 2020, pp. 607-608.

[7] C. Song, L. Wang, Z. Chen, G. Goussetis, G. A. E. Vandenbosch and Y. Huang, "Wideband mmWave Wireless Power Transfer: Theory, Design and Experiments," 2023 17th European Conference on Antennas and Propagation (EuCAP), Florence, Italy, 2023, pp. 1-5.

[8] O. Zetterstrom, E. Pucci, P. Padilla, L. Wang and O. Quevedo-Teruel, "Low-Dispersive Leaky-Wave Antennas for mmWave Point-to-Point High-Throughput Communications," in IEEE Transactions on Antennas and Propagation, vol. 68, no. 3, pp. 1322-1331, March 2020.

[9] X. Li, J. Wang, G. Goussetis and L. Wang, "Circularly Polarized High Gain Leaky-Wave Antenna for CubeSat Communication," in IEEE Transactions on Antennas and Propagation, vol. 70, no. 9, pp. 7612-7624, Sept. 2022.

[10] R. Bashirullah and A. Mortazawi, "A slotted-waveguide power amplifier for spatial power-combining applications," in IEEE Transactions on Microwave Theory and Techniques, vol. 48, no. 7, pp. 1142-1147, July 2000.

[11] Xin Jiang, Li Liu, S. C. Ortiz, R. Bashirullah and A. Mortazawi, "A Ka-band power amplifier based on a low-profile slotted-waveguide power-combining/dividing circuit," in IEEE Transactions on Microwave Theory and Techniques, vol. 51, no. 1, pp. 144-147, Jan. 2003.

[12] Xin Jiang, S. C. Ortiz and A. Mortazawi, "A Ka-band power amplifier based on the traveling-wave power-dividing/combining slotted-waveguide circuit," in IEEE Transactions on Microwave Theory and Techniques, vol. 52, no. 2, pp. 633-639, Feb. 2004.

[13] L. A. Li, B. J. Hilliard, J. R. Shafer, J. Daggett, E. J. Dickman and J. P. Becker, "A Planar Compatible Traveling-Wave Waveguide-Based Power Divider/Combiner," in IEEE Transactions on Microwave Theory and Techniques, vol. 56, no. 8, pp. 1889-1898.

[14] A. Sanada, K. Fukui and S. Nogi, "A waveguide type power divider/combiner of double-ladder multiple-port structure," in IEEE Transactions on Microwave Theory and Techniques, vol. 42, no. 7, pp. 1154-1161, July 1994.

[15] A. Sanada, K. Fukui, S. Nogi and M. Sanagi, "Traveling-wave microwave power divider composed of reflectionless dividing units," in IEEE Transactions on Microwave Theory and Techniques, vol. 43, no. 1, pp. 14-20, Jan. 1995.

[16] J. A. García-Pérez, G. Goussetis and S. Kosmopoulos, "1-to-4 double-side slotted waveguide power divider/combiner for Ka-band power amplifiers," 2015 SBMO/IEEE MTT-S International Microwave and Optoelectronics Conference (IMOC), Porto de Galinhas, Brazil, 2015, pp. 1-4.